



## Structural and some physical properties of Sodium Boro-phosphate Glass Containing Mill Scale.



CrossMark

A. S. El-Sayed<sup>a</sup>, A. G. Mostafa<sup>b</sup>, W.E.Madcour<sup>c</sup>, M. Y. Hassaan<sup>b</sup>

<sup>a</sup>Egyptian Metrological Authority, Cairo, Egypt.

<sup>b</sup>Phys. Dept., Faculty of Science, Al-Azhar University, Nasr City, Cairo, Egypt.

<sup>c</sup>N.R.C., Egyptian Atomic Energy Authority, Cairo, Egypt

### Abstract

Sodium boro-phosphate glasses containing different amounts of mill scale (65% FeO and 35% Fe<sub>2</sub>O<sub>3</sub>) [an iron industry waste formed during the rolling process to produce steel plates] were prepared by the melt quenching technique. The structure and some physical properties of the prepared glasses were investigated using different tools. The amorphous phase of the prepared glass samples was confirmed from their X-ray diffraction. The experimental and empirical densities were found to increase, while the experimental and empirical molar volumes were found to decrease, as mill scale content was increased. By comparing both the experimental and empirical values of density and molar volume, the amorphous nature and short range order character of the studied glasses was confirmed. It was found also that all glass samples behave like semiconductor and both electronic and ionic conductivities were present in these glasses. The correlated barrier hopping model is the appropriate conduction mechanism. The conductivity was found to increase as mill scale content was increased from 10 to 25 mol%, then decreased at sample contains 30 mol% of mill scale, The IR analysis indicated that the iron cations occupy the glass network modifier positions, while the iron cations occupies the glass network former positions only in the sample containing 30 mol% of mill scale. It indicated also that phosphorous cations occupy mainly the tetrahedral coordination state. The volume, mass and molar magnetic susceptibility measurements exhibited gradual increase as mill scale content was increased in the sample composition and all the samples exhibit paramagnetic character. © 2020 NIODC. All rights reserved

*Keywords:* Iron Industry Waste; Glass; Density; Molar volume; FTIR; XRD; Conductivity and Magnetic Susceptibility.

### 1. Introduction

Nowadays, attention is being drowned to investigate different glasses as useful solid materials, especially those containing transition metal cations [1]. It is well known early that, boron and phosphorus were considered as an important glass former cations that can be used in the preparation of glasses for both scientific and technological applications. The addition of alkali oxides may improve the physical properties of glasses and can modify their preparation conditions. Sodium has important alkali cation as well as iron is the most important transition metal. However, the study of the structural role of iron is also of interest due to its effect on the different properties of the produced. Such as their effects on chemical durability

[2], physical properties, electrical and magnetic properties [3,4]. Mill scale is an iron industry waste, which formed from the outer surfaces of the iron plates, sheets or profiles when they are being produced by rolling from the red-hot iron or steel. It consists mainly of 65% and 35%, FeO and Fe<sub>2</sub>O<sub>3</sub> respectively, and it is usually less than 1 mm thickness. Initially, it adheres to the steel surface, acting to protect it from atmospheric corrosion provided no break occurs in this coating layer [5]. Because it is electro-chemically cathodic to steel, any break in the mill scale coating will cause accelerated corrosion of steel exposed at this break. Mill scale is thus a boon for a while until it breaks due to handling of iron and steel products or due to any other mechanical stresses, where it was

\*Corresponding author e-mail: [ahmedsayed\\_phy@yahoo.com](mailto:ahmedsayed_phy@yahoo.com); (Ahmed Sayed El Sayed).

Receive Date: 18 March 2021, Revise Date: 04 May 2021, Accept Date: 06 June 2021

DOI: 10.21608/EJCHEM.2021.68425.3494

©2021 National Information and Documentation Center (NIDOC)

found that, it accumulated in the environment with huge amounts [6]. However, it was proposed that mill scale can be introduced as an iron industrial waste (which is formed only of iron oxides) into borophosphate glasses networks as an alternative raw material instead of pure iron oxide. Therefore, in this work, the glass formation and structure as well as physical properties of some sodium boro-phosphate glasses containing different proportions of mill scale will be thoroughly investigated. XRD and IR spectroscopy will be applied to confirm amorphous nature and to clarify the structural groups comprising the glass network. Also, measurements of density, molar volume, magnetic susceptibility and ac conductivity will be used for all the studied glass samples.

## 2. Experimental

Sodium boro-phosphate glass samples containing different amounts of mill scale were prepared by the melt quenching method. The composition of the glass samples was as the following:

[(40- 0.5x) B<sub>2</sub>O<sub>3</sub> . (40-0.5x) P<sub>2</sub>O<sub>5</sub> . 20 Na<sub>2</sub>O . (x) mill scale] mol %

Where x= (10, 15, 20, 25 and 30) mol%. Each batch, after mixing was melted in porcelain crucibles for two hrs. in an electrically heated furnace at 1450 K. Then, they were poured on a preheated stainless steel plate. The produced glass samples were measured by XRD to confirm the glassy state A perken Elmer (FTIR) spectrometer, model RTX, FTIR was used to collect the IR spectra in the vibrational range from 4000 to 400 cm<sup>-1</sup>, applying the KBr disk method. Archimedes method was used to obtain the experimental density values using CCl<sub>4</sub> as an immersion liquid having a stable density (1.59 g.cm<sup>-3</sup>) at RT. Then the density was calculated according to Archimedes formula [7]:

$$\rho_{\text{exp}} = \left( \frac{w_a}{w_a - w_{\text{CCl}_4}} \right) * \rho_{\text{CCl}_4} \quad (1)$$

where  $\rho_{\text{exp}}$  is the experimental density of the glass sample  $w_a$  is the weight of the sample in air.  $w_{\text{CCl}_4}$  the weight of the sample in CCl<sub>4</sub>.  $\rho_{\text{CCl}_4}$  is the density of CCl<sub>4</sub>.

Also the empirical density (the close packed structural density) will be also calculated by using the formula [8,9] :

$$\rho_{\text{emp}} = \sum \rho_j \cdot P_j \quad (2)$$

where  $\rho_{\text{emp}}$  is the empirical density of a glass, and  $\rho_1, \rho_2, \rho_3, \dots, \rho_j$  are the densities of the constituting oxides and  $p_1, p_2, p_3, \dots, p_j$  are the percentage weights of the composing oxides. Hence, both the experimental and the empirical densities will be plotted in the same Figure versus mill scale content for compression.

The experimental molar volume ( $V_m$ ) values of the studied glasses were also calculated using the following equation, [10]

$$\frac{\sum m_i c_i}{\rho} V_m = \quad (3)$$

Where,  $m_i$  is the mean molecular weight of a glass sample, and  $c_i$  is the percentage of the amount of such component and ( $\rho$ ) is the experimentally measured density. The empirical molar volume can be obtained by using the same equation .3 but with replacing the experimental density with the empirical one that calculated of a glass sample [9].

The a.c. measurements were carried out using a computer controlled Stanford LCR bridge model SR 720 at three fixed frequencies [ 1, 10, 100 kHz]. The investigated samples were ground and polished to obtain optically flat disk shape samples of 8 mm diameter and 2 mm thickness. Then, the obtained disks were painted by an air drying silver paste to ensure good electrical contact. All measurements were taken in the temperature range from 300 to 575 K.

The magnetic susceptibility of the investigated samples was studied and the volume magnetic susceptibility ( $K_v$ ) of all glasses was obtained by applying Gouy method. The change in the weights of the studied samples with the variation of the applied magnetic field were measured and then ( $K_v$ ) can be calculated by using equation (4) [11],

$$K_v = \left( \frac{2g}{a} \right) \left( \frac{\Delta m}{dH^2} \right) \quad (4)$$

Where ( $g$ ) is the acceleration due to gravity,  $a$  is the cross sectional area of the measured sample,  $\Delta m$  is the change in the weight of a glass samples and  $dH$  is the change in the applied magnetic field.

The mass magnetic susceptibility ( $M$ ) can be calculated by using equation (5),

$$m = kv/\rho \quad (5)$$

where  $\rho$  is the measured apparent density of a glass sample.

The molar magnetic susceptibility ( $\varphi$ ) can be obtained by applying equation (6),

$$\varphi = M \cdot W \quad (6)$$

where,  $W$  is the mean molecular weight of the glass sample under investigation [12,13].

### 3. Results and discussion

Firstly, it was tried many time to prepare a glass sample free of mill scale but these trials were not give glass, since the obtained ones appeared to be highly hygroscopic and absorb environmental moisture from air. When 5mol% of mill scale was introduced, it was give glass but not stable, when 10mol% of mill scale was introduced the durability of the prepared glasses appeared to be enhanced enough. Therefore, five samples were prepared containing different amounts of mill scale, and their chemical composition as well as their nomination are shown in table (1) It should be noted that (NH<sub>4</sub>H<sub>2</sub>PO<sub>4</sub>) was used to obtain P<sub>2</sub>O<sub>5</sub>

Table (1), Compositions and nominations of the studied glasses.

No	Nomination	Composition
1	P10 ms	[35% B <sub>2</sub> O <sub>3</sub> , 35% P <sub>2</sub> O <sub>5</sub> , 20% Na <sub>2</sub> O, 10% mill scale]
2	P15 ms	[32.5% B <sub>2</sub> O <sub>3</sub> , 32.5% P <sub>2</sub> O <sub>5</sub> , 20% Na <sub>2</sub> O, 15% mill scale]
3	P20 ms	[30% B <sub>2</sub> O <sub>3</sub> , 30% P <sub>2</sub> O <sub>5</sub> , 20% Na <sub>2</sub> O, 20% mill scale]
4	P25 ms	[27.5% B <sub>2</sub> O <sub>3</sub> , 27.5% P <sub>2</sub> O <sub>5</sub> , 20% Na <sub>2</sub> O, 25% mill scale]
5	P30 ms	[25% B <sub>2</sub> O <sub>3</sub> , 25% P <sub>2</sub> O <sub>5</sub> , 20% Na <sub>2</sub> O, 30% mill scale]

#### 3.1. XRD Results

The obtained XRD spectra of sample containing 10 mol% is exhibited in Fig. (1) as a representative figure. The pattern showed fluctuations and no sharp peaks were found which confirm the amorphous nature of the prepared glass samples.

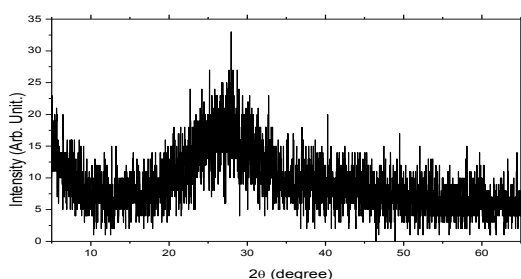


Fig. (3) The obtained XRD pattern of sample containing 10mol% mill scale as a representative pattern.

#### 3.2. Density and molar volume results:

Since density is a property of interest, where it relates directly to many other physical properties were it can be used to calculate many physical parameters. However, Archimedes method was applied to the experimental density measurements ( $\rho_{exp}$ ), The empirical density ( $\rho_{emp}$ ) was also calculated. Fig (2) represents the variation of both ( $\rho_{exp}$ ) and ( $\rho_{emp}$ ) for the studied glasses as mill scale was gradually increased up to 30 mol%. This figure showed that both density values increased linearly, where this may be due to the higher density of mill scale (5.565 g/cm<sup>3</sup>) than that of phosphorus penta-oxide (2.39 g/cm<sup>3</sup>) and boron oxide (2.46 g/cm<sup>3</sup>), in addition to, iron atoms enter as former cations and the other enter as modifier cations. It is noticed that,  $\rho_{exp}$  exhibits as usual lower values than the corresponding  $\rho_{emp}$  values. This indicated that all the studied glass samples exhibit amorphous nature and short range order character [14,15].

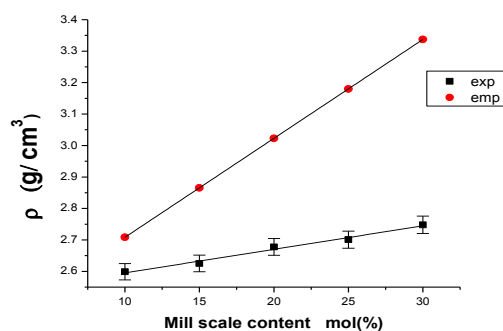


Fig. (2), The relation between both the experimental and empirical densities versus mill scale content.

Since the molar volume of a glass sample is directly related to the internal spatial structure of such samples, therefore, the variation of both the experimental and empirical molar volume values with mill scale content were drawn in Fig. (3).

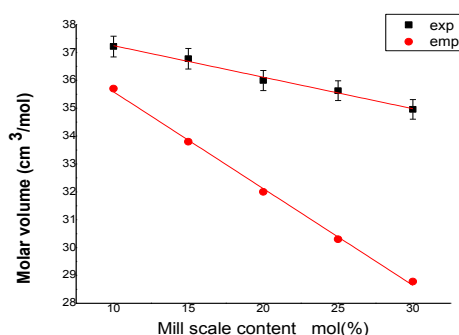


Fig. (3) The variation of both the empirical and experimental molar volume versus mill scale content.

It is seen that, both  $(V_m)_{exp}$  and  $(V_m)_{emp}$  were decreased linearly, and the empirical values are lower than the corresponding experimental ones. This also confirmed the results of the density (experimental and empirical).

Also, the observed divergence between the rate of change of both the empirical and experimental values of both density and molar volume may indicate that as mill scale was gradually increased the stability of the studied glasses increased. This confirms the amorphous phase of all glasses and it reveals that, mill scale ( $Fe_2O_3$  &  $FeO$ ) is highly dissolved in the prepared boro-phosphate networks [16].

The observed increase in density and decrease in molar volume can be attributed to the supposition that, as mill scale content was gradually increased into the glass network at the expense of  $P_2O_5$  and  $B_2O_3$ , some iron cations may occupy the glass network former (GNF) positions while some others may occupy the glass network modifier (GNM) positions. This means that the cations of iron that acted as GNM occupies the interstitial positions and hence decreased the network vacancies.

### 3.3. a.c. conductivity results:

The frequency dependent conductivity has been observed in many amorphous solids and glasses specially those containing transition metal ions (TMI). The importance of the role of transition metal ions is due to the capability of existing in more than one valence state. So the conduction can take place by electron hopping between both valence states from the lower state to the higher one according to Mott [17], in addition to the presence of alkali cations that cause ionic conduction. The frequency dependence conductivity for many amorphous solids and glasses was found to follow the universal power law,

$$\sigma(\omega) = A \omega^s \quad (7)$$

Where,  $\sigma(\omega)$  is the ac conductivity, (A) is a weakly temperature dependent factor,  $\omega$  is the angular frequency and (s) is the exponent factor (usually less than unity).

The conduction can take place by hopping or tunneling of electrons and the mobile charge carrier ions between the occurred equilibrium sites [18].

The obtained  $\ln[\sigma(\omega)]$  as a function of  $(1/T)$  and at only three fixed frequencies [1, 10, 100 kHz], are exhibited in Fig. (4) for the sample containing 10 mol% mill scale as a representative sample, and all samples showed similar behavior. From all relation it can be seen generally that  $\ln[\sigma(\omega)]$  increases with

increasing temperature, this means all the samples behave like semiconductor. It can be stated also that,  $\ln[\sigma(\omega)]$  showed weak temperature dependence and strong frequency dependence at relatively low temperatures, while at relatively high temperatures, it showed strong temperature dependence and weak frequency dependence. At low temperatures, the a.c. conductivity is suggested to be mainly due to electron hopping between two sites in the localized states ( $Fe^{2+}$  and  $Fe^{3+}$ ). while at higher temperatures,  $\ln[\sigma(\omega)]$  is suggested to be thermally activated processes.

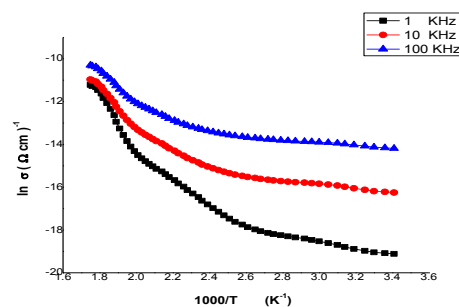


Fig (4),  $\ln(\sigma)$  vs.  $1/T$  of the sample containing 10% mill scale as a representative sample.

The variation of the measured dielectric constant ( $\epsilon$ ) as a function of temperature at three fixed frequencies [1, 10, 100 kHz], are shown in Fig. (5), for the sample containing 10 mol% mill scale as a representative sample, and all samples showed approximately similar behavior. It can be seen that ( $\epsilon$ ) appeared to be approximately stable with increasing the temperature, up to certain temperature ( $T_0$ ) at which it started to increase gradually. The value of ( $T_0$ ) was found to vary from sample to another as well as with the change of frequency where it increased with the increasing of frequency. That is to say, at low temperatures, the change in ( $\epsilon$ ) is almost independent on both temperature and frequency, while at high temperatures ( $\epsilon$ ) is strongly dependent on both temperature and frequency. This means that the internal electric field is in phase with the external one, so the movement of the electric dipoles increased [19].

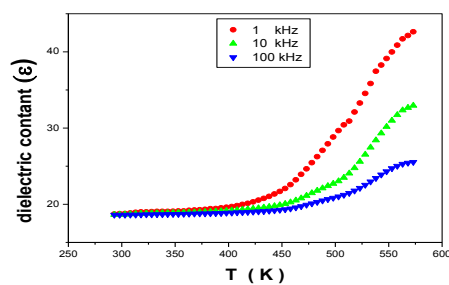


Fig (5) the variation of the dielectric constant of the sample containing 10mol% mill scale vs. T as a representative sample.

The measured dielectric loss ( $\epsilon''$ ) as a function of temperature for all samples showed approximately similar behavior, and Fig (6) exhibits the variation of ( $\epsilon''$ ) as the temperature was gradually increased, for the sample containing 10 mol% mill scale as a representative sample. It appeared also that, at low temperatures, ( $\epsilon''$ ) is almost independent on both frequency and temperature, while at high temperatures,  $\epsilon''$  is strongly dependent on temperature and frequency. This means that the energy loss due to the frictions that take place during the movement of the dipoles increased and the dielectric loss increased.

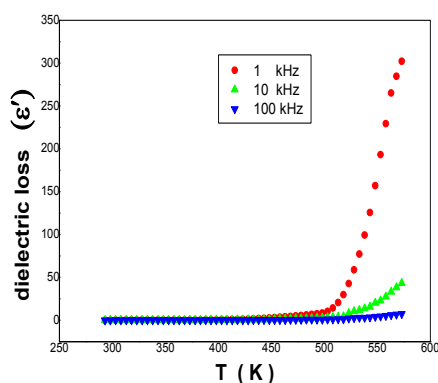


Fig (6) the variation of the dielectric loss vs. T for the sample containing 10mol% mill scale as a representative sample.

Inspecting the conduction mechanism in these glasses, the exponent factor (s) was calculated from equation (8), and plotted as a function of temperature,

$$s = d \ln [\sigma (\omega)] / d \ln [\omega] \quad \text{-----} (8)$$

However, Fig (7) shows the change of the calculated (s) values when plotted as a function of temperature, for the sample that contained 10 mol% mill scale, as a representative sample. From this Figure, it appeared that the factor (s) is frequency and temperature dependent, and it decreased gradually with increasing temperature. It was tried to fit the experimentally obtained data of (s) factor with the theoretical equations of different models, the best fit was clearly obtained when applying the correlated Barrier hopping (CBH) model (equation (9)),

$$s = 1 - \frac{6KT}{w+KT \ln(\omega t_0)} \quad (9)$$

Fig. (8), exhibits the change in conductivity as a function of mill scale concentration, at 100° C and different three frequencies 1, 10, 100 kHz where a gradual increase was clearly observed as mill scale was increased from 10 to 25 mol% because of the increase of iron ions that behaved as modifier. The sample contains 30 mol% of mill scale the

conductivity decreased, the reason of decreasing conductivity may be due to the entrance of mill scale in the network as former so the number of free ions decreased. Accordingly, the studied glass samples should be examined by IR spectroscopy, in order to decide exactly the reason for the decrease in conductivity of the sample containing 30 mol% of mill scale.

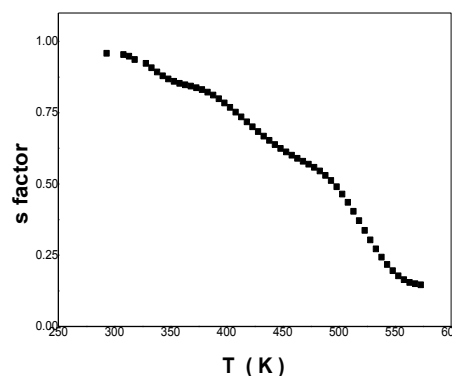


Fig (7) The variation of (s) factor vs. T for the sample containing 10mol% mill scale as a representative sample.

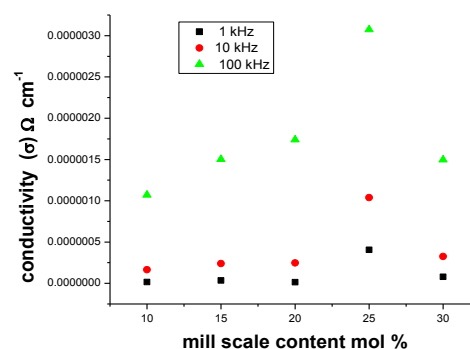


Fig. (8) the variation of the conductivity as mill scale content was increased.

### 3.4. IR Results:

The obtained IR spectra of the measured samples are exhibited in Fig. (9), in the region from 4000 to 400  $\text{cm}^{-1}$ . From this Figure, it appeared that, the range above 2000 up to 4000  $\text{cm}^{-1}$ , comprises only some bands due to H-O-H and O-H vibrations. the band appeared around 1600  $\text{cm}^{-1}$  can be attributed to the bending vibration of molecular water. So the range of interest in this study was insisted only in between 400 up to about 1600  $\text{cm}^{-1}$ .

Then the deconvolution program was applied to all the obtained IR spectra, in the range of interest, in order to confirm the exact wavenumber of the supposed vibrational energies as supplied by the apparatus. However, Fig. (10) exhibits the de-

convoluted spectrum of the sample containing 10 mol% mill scale, as a representative sample. The attributions of the analyzed bands for all the IR spectra of the studied glasses are summarized in Table (2).

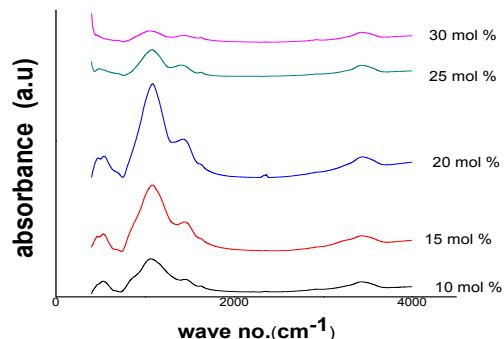


Fig (9) The obtained IR spectrum of all samples.

Table (2) the obtained wave numbers of IR results

Bands no.	Mill scale content mol%				
	10	15	20	25	30
1	427	408	431	396	400 410
2	460	455	468	471	-----
3	529	528	542	591	623
4	683	683	638	708	701
5	821	819	872	847	-----
6	891	890	998	980	903
7	1019	1005	1080	1101	1043
8	1147	1125	1158	1192	1168
9	1321	1317	1309	1311	1274
10	1466	1465	1455	1441	1420

1. The absorption bands at (396 - 431)  $\text{cm}^{-1}$  is assigned to be due to the vibrations of  $(\text{P}_2\text{O}_7)^{4-}$  groups ( $\text{Q}^1$  groups) [20], or can be related to vibrations of Na ions in their modifying sites [21].

2. The absorption bands at (455-471)  $\text{cm}^{-1}$  is assigned to be due to iron ions in the octahedral coordination state ( $\text{FeO}_6$ ) occupying GNM Positions [22].

3. The absorption bands at (528-623)  $\text{cm}^{-1}$ , the band between 528 and 591  $\text{cm}^{-1}$  corresponds to the bending mode of O-P-O in the  $\text{Q}^1$  structure, the band 623

$\text{cm}^{-1}$  can be attributed to the stretching band of the Fe-O-P bond [23].

4. The absorption bands at (638-708)  $\text{cm}^{-1}$  can be attributed to bending vibrations of B-O linkages in  $[\text{BO}_4]$  [24,25].

5. The absorption bands at (819-872)  $\text{cm}^{-1}$  is assigned to the antisymmetric stretching vibrations of P-O-P bonds in  $[\text{PO}_2]$  groups [24].

6. The absorption bands at (890-998)  $\text{cm}^{-1}$  can be attributed to the stretching vibrations of  $[\text{BO}_4]$  [24,26,27].

7. The absorption bands at (1005-1101)  $\text{cm}^{-1}$  can be attributed to the vibrations of  $\text{PO}_4^{-3}$  groups ( $\text{Q}^0$  groups) [28,29,30].

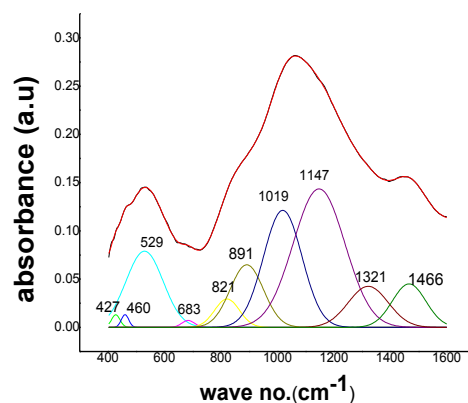


Fig (10) The de convoluted IR spectra of the sample containing 10mol% mill scale as a represented figure

8. The absorption bands at (1125-1192)  $\text{cm}^{-1}$  are corresponding to the  $(\text{PO}_3)^-$  groups ( $\text{Q}^2$  groups) and the symmetric stretching vibrations of O-P-O bonds [31], the peak at 1168 can be considered as the stretching vibrations of Fe-O-P bonds [28].

9. The absorption bands at (1274-1321)  $\text{cm}^{-1}$ , the peak at 1274 can be considered as the stretching vibrations of Fe-O-P bonds [28], the band between (1309 -1321) are corresponding to the symmetric stretching vibrations of P=O bonds [28, 31].

10. The absorption bands at (1420-1466)  $\text{cm}^{-1}$  are corresponding to the vibration modes of  $[\text{BO}_3]$  and  $\text{BO}_2\text{O}^-$  [32].

The other bands observed at the wavenumbers higher than 1500  $\text{cm}^{-1}$  are related to the vibrations of H-O-H, POH, and BOH [7,32].

It appeared from the IR results that, many structural building groups and bond vibrations appeared in the glass networks. It can be stated also that the coordination of iron ( $\text{FeO}_6$ ) that occupying GNM positions are appeared in the spectrum of all samples, and the GNF positions (Fe-O-P) are appeared in the spectrum of sample contains 30 mol% of mill scale only.

### 3.5. Magnetic susceptibility Results:

The magnetic properties of the prepared glasses are a matter of interest especially when their networks include some transition metal cations. Among all transition metals, iron is the most effective element which affects greatly the magnetic and electrical properties of glasses. Since mill scale is composed only of ferrous and ferric oxides, therefore, Gouy method was applied here to measure the magnetic susceptibility of the studied glass samples [11]. Figure (11), represents the change in the weight of a glass sample ( $\Delta m$ ) as a function of the square of the magnetic field intensity due to the magnetic pull of the applied magnetic field. It appeared that,  $\Delta m$  values increased linearly as the magnetic field intensity was increased for all the studied glass samples.

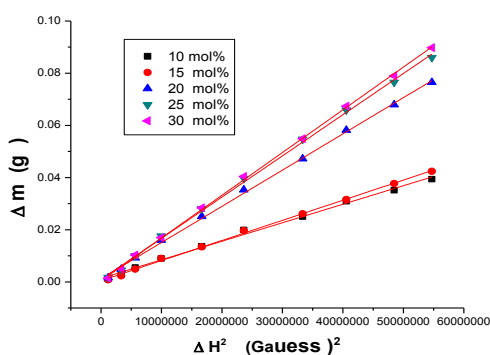


Fig. (11), The change in  $\Delta m$  as a function of  $\Delta H^2$ , for all samples.

The volume magnetic susceptibility ( $K_v$ ) was then calculated by applying equation (4), and the obtained values are exhibited in Table (3) as a function of mill scale (iron oxide) content. It appeared that, as mill scale was gradually increased, the volume magnetic susceptibility increased also.

Also, the mass of magnetic susceptibility ( $M$ ) was then calculated by applying equation (5), and the obtained values are listed also in Table (3) as a function of mill scale content, where it exhibits approximately the same trend that exhibited by the volume susceptibility.

Since the molar magnetic susceptibility ( $\phi$ ) represents the normalized susceptibility values, therefore, they were also calculated by using equation (6) and were also plotted in Fig.(12) as a function of mill scale content.

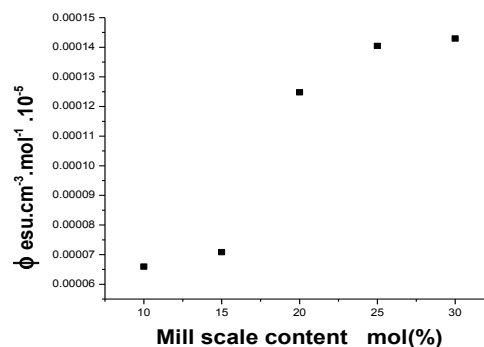


Fig. (12), The change in  $\phi$  versus mill scale content.

Table (3) The magnetic susceptibility values ( $K_v$  in  $\text{esu} \cdot 10^{-6}$ ,  $M$  in  $\text{esu} \cdot \text{cm}^3 \cdot \text{gm} \cdot 10^{-7}$  and  $\phi$  in  $\text{esu} \cdot \text{cm}^3 \cdot \text{mol}^{-1} \cdot 10^{-5}$ ).

mill scale content mol%	10	15	20	25	30
$K_v$	1.8	1.93	3.491	3.924	4.1
$M$	6.92	7.37	13.04	14.53	14.91
$\phi$	4.71	5.14	9.307	10.61	11.14

Inspecting the obtained results presented in table (3), it is easy to observe that, all the obtained susceptibilities increased gradually as mill scale content were gradually increased. Such increase may be due to the gradual increase of mill scale i.e. iron cations.

### 4. Conclusion

The present work is devoted to study the effect of mill scale in a glass system of chemical composition  $[(40-0.5x) \text{B}_2\text{O}_3 \cdot (40-0.5x) \text{P}_2\text{O}_5 \cdot 20\% \text{Na}_2\text{O} \cdot (x) \text{mill scale}] \text{ mol } \%$ . Where  $x = (10, 15, 20, 25 \text{ and } 30) \text{ mol } \%$ . XRD pattern confirm the glass formability of the prepared samples. The density is found to be increased and molar volume is found to be decreased by increasing mill scale content. From the a.c. conductivity measurements, it can be concluded that all glass samples behave like semiconductor and the correlated barrier hopping (CBH) model is applicable mechanism. The a.c. conductivity is found to be increased by increasing mill scale content. From IR measurements it can be stated that the iron cations occupying GNM positions are appeared in the spectrum of all samples, and the GNF positions are appeared in the spectrum of sample contains 30 mol% of mill scale only. From magnetic susceptibility measurements it can be concluded that, all the obtained susceptibility values increased gradually as mill scale content were gradually increased.

#### 4. References

- P.Y. Shin, S.W.Yung and T.S.Chin, *J. Non-Crystalline Solids*, 244, (1999), 211.
- A.A. Ramadan, A.G. Mostafa, M.Y. Hassaan, A.Z. Hussein and A.Y. Abdel-Haseib, *Isotope & Rad. Res.*, 46 (1), (2014) 83.
- Y.A. Elbasha, M. Ibrahim Ali, H.A. Elshaikh and Ahmed Gamal El-Din Mostafa, *Optik*, 127 (2016) 7041.
- G.S.M. Ahmed, A.S. Mahmoud, S.M. Salem and T. Z. Abou-Elnasr, *American J. Phys. & Applications*, 3 (4), (2015) 112.
- T.Umadevi, M.G. Sampath Kumar and P.C. Mahapatra, *Ironmak.Steelmak.*, 36(6), (2009) 409.
- E.Mahallati SM., *Cem. Concr. Res.*, 36(2006) 1324.
- F.H. ElBatal, S. Ibrahim, A.M. Abdelghany, *Journal of Molecular Structure* 1030 (2012) 107–112.
- U.B. Chanshetti, V.A. Shelke., S.M. Jadhav, S.G. Shankarwar, T.K. Chondhekar, A.G. Shankarwar, V.Sudarsan and M.S. Jogad, *Facta Univ. –Ser Physics, Chem.Technol.*, 9(1)(2011)29.
- A.M. Abdel-Ghany, A.A. Bendary, T.Z. Abou-Elnasr, M.Y. Hassan and A.G. Mostafa, *Nat.& Sci.*, 12(6), (2014)139.
- VirenderKundu, R. L. Dhiman, A. S. Maan, and D. R. Goyal, *Advances in Condensed Matter Physics Volume* (2008), Article ID 937054, 7 pages.
- Ahmed Gamal El-Din Mostafa, *Turk. J. Phys.*, 26 (2002) 441
- Gamal El-DeenAbd El-RaheemYAHYA, *Turk J Phys* 27 (2003), 255 – 262.
- Mohamed Gabr, Karam Abdel-Aati Ali, and Ahmed Gamal El-Din Mostafa., *Turk. J. Phys.*, 31, (2007) 31.
- A.M. Abdel-Ghany, M.S.S. Saad, I.I.Bashter, T.Z. Amer, S.M. Salam and A.G. Mostafa. *Nat Sci.*, 12(12), (2014) 162.
- H.A. Saudi, A. Abd-Elalim, T.Z. Abou-Elnasr and A.G. Mostafa, *American J. Phys. And Applications*, 13(11), (2015)139.
- A.M. Zoulfakar, A.M. Abdel-Ghany, T.Z. Abou-Elnasr, A.G. Mostafa, S.M. Salem, H.H. El-Bahnaswy, *J.Applied Radiation and Isotopes*, 127 (2017) 269.
- N.F. Mott, E.A. Davis: *Electronic Processes in Non-Crystalline Materials* 2nd ed. Clarendon, Oxford (1979)
- E. I. Kamitsos, A. P. Patris, M. A. Karakassides & G. D. Chryssikos, *J. Non-Cryst. Solids*, 126, 52 (1990).
- Leonard Dissado: *Springer Handbook of Electronic and Photonic Materials*, 2nd edition, 2017.
- Q. Liao, F. Wang, K. Chen, S. Pan, H. Zhu, M. Lu, J. Qin, 1092 (2015) 187-191.
- F. H. A. Elbatal, M. A. Marzouk, Y. M. Hamdy, and H. A. ElBatal, *Journal of Solid State Physics*, 389543, 2014.
- [Bin Qiana, Xiaofeng Liang, Shiyuan Yang, Shu He, Long Gao, *Journal of Molecular Structure* 1027 (2012) 31–35.
- Bin Qian, Shiyuan Yang, Xiaofeng Liang, Yuanming Lai, Long Gao, Guangfu Yin, *Journal of Molecular Structure* 1011 (2012) 153–157.
- F.H. ElBatal, S. Ibrahim, A.M. Abdelghany, *J. Mol. Struct.* 1030 (2012) 107-112.
- D. Toloman, A.R. Biris, D. Maniu, I. Bratu, L.M. Giurgiu, A.S. Biris, I. Ardelean, *Particulate Sci. Technol.* 28 (2010) 226-235.
- E.I. Kamitsos, A. Patsis, G.D. Chryssikos, *J. Non-Cryst. Solids* 152 (1993) 240-257.
- K. Srinivasulu, I. Omkaram, H. Obeid, A. Suresh Kumar, J.L. Rao, *J. Mol. Struct.* 1036 (2013) 63-70.
- D.A. Magdas, O. Cozar, V. Chis, I. Ardelean, N. Vedeanu, *Vib. Spectrosc.* 48 (2008) 251-254.
- P. Subbalakshmi, N. Veeriah, *J. Non-Cryst. Solids* 298 (2002) 89-98.
- Y.M. Moustafa, A. El-Adawy, *Phys. Stat. Sol. A* 179 (2000) 83-93.
- L. Baia, D. Muresan, M. Baia, J. Popp, S. Simon, *Vib. Spectrosc.* 43 (2007) 313-318.
- A.M Abdelghany, M.A. Ouis, M.A. Azooz, H.A. ElBatal, *Spectrochim. Acta, Part A* 114 (2013) 569-574.